Prdm16 is a critical regulator of adult long-term hematopoietic stem cell quiescence

Kristbjorn O. Gudmundsson[a,1], Nhu Nguyen[a], Kevin Oakley[a], Yufen Han[a], Bjorg Gudmundsdottir[b], Pentao Liu[c], Lino Tessarollo[d], Nancy A. Jenkins[e], Neal G. Copeland[e,2], and Yang Du[a,2]

[a]Department of Pediatrics, Uniformed Services University of the Health Sciences, Bethesda, MD 20814; [b]Cellular and Molecular Therapeutics Branch, National Heart Lung and Blood Institute, National Institutes of Health, Bethesda, MD 20814; [c]School of Biomedical Sciences, The University of Hong Kong, Pokfulam, Hong Kong; [d]Mouse Cancer Genetics Program, Center for Cancer Research, National Cancer Institute, Frederick, MD 21702; and [e]Department of Genetics, The University of Texas MD Anderson Cancer Center, Houston, TX 77030

Contributed by Neal G. Copeland, October 28, 2020 (sent for review August 20, 2020; reviewed by Adam N. Goldfarb and Paul Liu)

Regulation of quiescence is critical for the maintenance of adult hematopoietic stem cells (HSCs). Disruption of transcription factor gene *Prdm16* during mouse embryonic development has been shown to cause a severe loss of fetal liver HSCs; however, the underlying mechanisms and the function of *Prdm16* in adult HSCs remain unclear. To investigate the role of *Prdm16* in adult HSCs, we generated a novel conditional knockout mouse model and deleted *Prdm16* in adult mouse hematopoietic system using the IFN-inducible *Mx1-Cre*. Our results show that *Prdm16* deletion in the adult mouse hematopoietic system has a less severe effect on HSCs, causing a gradual decline of adult HSC numbers and a concomitant increase in the multipotent progenitor (MPP) compartment. *Prdm16* deletion in the hematopoietic system following transplantation produced the same phenotype, indicating that the defect is intrinsic to adult HSCs. This HSC loss was also exacerbated by stress induced by 5-fluorouracil injections. Annexin V staining showed no difference in apoptosis between wild-type and knockout adult HSCs. In contrast, Bromodeoxyuridine analysis revealed that loss of *Prdm16* significantly increased cycling of long-term HSCs (LT-HSCs) with the majority of the cells found in the S to G2/M phase. Consistently, RNA sequencing analysis of mouse LT-HSCs with and without *Prdm16* deletion showed that *Prdm16* loss induced a significant decrease in the expression of several known cell cycle regulators of HSCs, among which *Cdkn1a* and *Egr1* were identified as direct targets of *Prdm16*. Our results suggest that *Prdm16* preserves the function of adult LT-HSCs by promoting their quiescence.

hematopoietic stem cells | Prdm16 | quiescence

Cell cycle control plays an important role in maintaining adult hematopoietic stem cells (HSCs). Adult HSCs are largely quiescent, and increased cycling has been thought to cause their loss by inducing premature differentiation. In support of this notion, gene ablation studies in mice have shown that cell cycle inhibitors, particularly cyclin-dependent kinase (CDK) inhibitors including CDKN1A (p21) and CDKN1C (p57), are critical for the maintenance of adult HSCs (1, 2). A number of transcription factors known to be essential for HSC maintenance, such as *Gfi1*, *Pbx1*, and *Mecom*, were also found to negatively regulate their proliferation (3–5). Elucidating the molecular mechanisms governing adult HSC quiescence will greatly enhance our capability to harness the power of these cells in regenerative medicine. However, the current understanding of the regulation of HSC quiescence in response to various intrinsic and extrinsic signals remains very limited and will be significantly advanced by identifying additional pathways and regulators.

PRDM16 encodes a zinc-finger transcription factor homologous to MECOM and was first cloned from chromosome translocations in myelodysplastic syndrome (MDS) and acute myeloid leukemia (AML) patients (6). Two major isoforms of PRDM16 protein have been reported due to usage of different transcriptional start sites: a longer variant containing the N-terminal PR domain, which is homologous to the SET domain found in lysine methyltransferases and has been shown to methylate H3K4 and H3K9 (7, 8), and a shorter variant that lacks the PR domain (6). The same DNA-binding specificity is expected for the two isoforms, as both contain the entire 10 C2H2-type zinc fingers that are divided into two domains: the N-terminal DNA binding domain 1 (DBD1), containing seven zinc fingers, and the C-terminal DBD2, containing three zinc fingers. Increasing evidence in the leukemia field suggests that significant functional differences exist between the two isoforms. The chromosome rearrangements involving *PRDM16* in MDS and AML patients cause preferential activation over the full-length protein of the shorter isoform of PRDM16, which is also the only form capable of inducing myeloid leukemia development in mice (9). This shorter isoform of *Prdm16* is also preferentially activated by retroviral insertions causing immortalization of myeloid progenitors (10). Mechanistically, direct activation of *Spi1* by the shorter isoform has been recently shown to be critical for its transformation of megakaryocyte-erythroid progenitors into leukemia stem cells for AML development (11). In contrast, the full-length form has been shown to antagonize leukemia development through activating *Gfi1b* (8, 12).

Previous studies have also identified *Prdm16* as an important regulator for the generation/maintenance of fetal liver HSCs; however, the underlying mechanisms and the role of *Prdm16* in adult HSC function remain unclear. Homozygous mice for the *Prdm16* gene trap allele die shortly after birth, precluding analysis of the role of *Prdm16* in adult HSCs (13, 14). Although a *Prdm16*

Significance

Regulation of quiescence is critical for the maintenance of adult HSCs, and the underlying mechanisms are poorly understood. Using a novel mouse conditional knockout allele of transcription factor gene *Prdm16*, we show that its deletion in the adult hematopoietic system led to a gradual loss of adult HSCs over time. This loss of adult HSCs was associated with their significantly increased cycling. We further found that *Prdm16* promotes the quiescence of adult HSCs by activating the transcription of HSC cell cycle inhibitors including *Cdkn1a* and *Egr1*. Our study identifies *Prdm16* as a critical regulator of adult HSC quiescence.

Author contributions: K.O.G. and Y.D. designed research; K.O.G., N.N., K.O., Y.H., B.G., and Y.D. performed research; L.T. and N.A.J. contributed new reagents/analytic tools; K.O.G., N.N., K.O., Y.H., B.G., P.L., N.G.C., and Y.D. analyzed data; and K.O.G., N.G.C., and Y.D. wrote the paper.

Reviewers: A.N.G., University of Virginia; and P.L., National Institutes of Health.

The authors declare no competing interest.

[1]Present address: Basic Research Program, Leidos Biomedical Research Inc., Frederick National Laboratory for Cancer Research, Frederick, MD 21702.

[2]To whom correspondence may be addressed. Email: ncopeland1@mdanderson.org or yang.du@usuhs.edu.

This article contains supporting information online at https://www.pnas.org/lookup/suppl/doi:10.1073/pnas.2017626117/-/DCSupplemental.

First published December 2, 2020.

conditional allele was recently reported, *Vav-Cre* was used to induce hematopoietic-specific deletion (12). Due to the expression of *Vav-Cre* during fetal hematopoiesis, it is unclear whether the observed severe HSC defects in adult mice in this study are partly due to possible generation of abnormal adult HSCs in the absence of *Prdm16*.

To address the function of *Prdm16* in adult HSCs, we generated a different *Prdm16* conditional allele and deleted the gene in the hematopoietic system in adult mice using the inducible *Mx1-Cre* (15). In contrast to the acute loss of HSCs observed in previous studies, our results show that *Prdm16* deletion caused a gradual reduction in adult HSC numbers that was exacerbated under stress. Consistent with this phenotype, we found that *Prdm16* plays a critical role in maintaining the quiescence of adult HSCs. Downstream targets of *Prdm16* involved in this regulation also were identified.

Results

Generation of *Prdm16* Knockout and Conditional Alleles. To determine the role of *Prdm16* in adult HSCs, we generated a conditional allele of *Prdm16* through gene targeting in mouse embryonic stem (ES) cells. In order to completely knock out *Prdm16* function, two *loxP* sites were inserted sequentially before exon 6 and after exon 12 by two consecutive gene-targeting experiments in CJ7 mouse ES cells. This design allows removal of the entire first and 50% of the second zinc finger domain of *Prdm16*, the only two domains responsible for its DNA binding capability (*SI Appendix*, Fig. S1 *A* and *B*). Two ES cell clones harboring the doubly targeted *Prdm16* allele were confirmed by Southern blotting analysis and subsequently used for blastocyst injection. A *Prdm16* conditional allele was subsequently generated by breeding mice carrying the targeted allele with *ACTB-Flpe* mice to remove the neomycin and blasticidin resistance cassettes used for selection in ES cells. A *Prdm16* conventional knockout also was generated by crossing the targeted mice to *ACTB-Cre* mice. As expected, mice homozygous for the *Prdm16* conditional allele are healthy and fertile. In contrast, the homozygous *Prdm16* knockout mice die within 24 h of birth, likely due to cleft palate development. *Prdm16* messenger RNA (mRNA) was not detected by RT-PCR in fetal livers from e18.5 $Prdm16^{-/-}$ embryos (*SI Appendix*, Fig. S1*C*), nor was PRDM16 protein detected in fetal brain nuclear extracts isolated from e15.5 $Prdm16^{-/-}$ embryos (*SI Appendix*, Fig. S1*D*), confirming loss of *Prdm16* expression in the knockout animals.

***Prdm16*$^{-/-}$ Fetal Livers Have Severe Reduction of Long-Term HSCs.** Previous studies, using a *Prdm16* gene trap allele ($Prdm16^{LacZ}$), have shown that $Prdm16^{LacZ/LacZ}$ animals have severe reduction of fetal liver HSCs but grossly normal hematopoiesis with no significant changes in the frequency of myeloid, B, or T cells (13, 14). In agreement with the gene trap model, analysis of e18.5 fetal thymuses and livers from our $Prdm16^{-/-}$ embryos demonstrated that hematopoiesis was essentially normal, with similar frequencies of myeloid and B cells detected in fetal livers (*SI Appendix*, Fig. S2*A*) and of T cells detected in fetal thymuses (*SI Appendix*, Fig. S2*B*). Flow cytometry analysis showed that the frequency of the Lin-Sca-1$^+$c-Kit$^+$ (LSK) population enriched for HSCs was similar in the e18.5 $Prdm16^{-/-}$ livers in comparison to $Prdm16^{+/+}$ fetal livers (Fig. 1 *A* and *B*). More detailed analysis of the LSK compartment showed a significant increase in multipotent progenitors (MPPs), approximately fivefold reduction in short-term HSCs (ST-HSCs, Lin-Sca-1$^+$c-Kit$^+$CD48$^-$CD150$^-$) and over 50-fold reduction in long-term HSCs (LT-HSCs) (Lin-Sca-1$^+$c-Kit$^+$CD48$^-$CD150$^+$) in the $Prdm16^{-/-}$ fetal livers, indicating that the HSC compartment is severely compromised upon loss of *Prdm16* (Fig. 1 *A* and *B*). Similar to the e18.5 $Prdm16^{-/-}$ fetal livers, MPPs also were significantly increased and ST-HSCs and LT-HSCs were significantly decreased in e14.5 $Prdm16^{-/-}$ fetal livers (*SI Appendix*, Fig. S3 *A* and *B*). However, the reduction in LT-HSCs at e14.5 was not to the same extent as at e18.5 (*SI Appendix*, Fig. S3*C*), suggesting that LT-HSCs seed the liver normally and that the effects of *Prdm16* loss on LT-HSCs become apparent subsequently, most likely due to defects in HSC expansion which is essentially a continuous self-renewal cycle (16). Consistent with this hypothesis, e18.5 $Prdm16^{-/-}$ fetal liver cells expanded poorly in culture under a condition shown to promote self-renewal of LT-HSCs (*SI Appendix*, Fig. S4*A*) (17). Immature clonogenic cells also decreased rapidly in the $Prdm16^{-/-}$ culture over time (*SI Appendix*, Fig. S4*B*). To test the self-renewal capability of $Prdm16^{-/-}$ fetal liver HSCs in vivo, 1×10^6 fetal liver cells from e18.5 $Prdm16^{+/+}$ or $Prdm16^{-/-}$ embryos were competed against the same number of wild-type CD45.1$^+$ bone marrow cells after transplantation into lethally irradiated congenic *C57BL/6-Ly5.2* recipient mice. At 1-mo posttransplantation, the percentage of peripheral blood CD45.2$^+$ cells was significantly lower in the recipients of $Prdm16^{-/-}$ fetal liver cells than in mice receiving $Prdm16^{+/+}$ fetal liver cells (Fig. 1*C*). At 2, 6, and 12 mo, the percentage of CD45.2 cells was reduced even further in the recipients of $Prdm16^{-/-}$ fetal liver cells (Fig. 1*C*). Analysis of the HSC compartment further showed a complete loss of $Prdm16^{-/-}$ LT-HSCs in the recipients of $Prdm16^{-/-}$ fetal liver cells at 12 mo (*SI Appendix*, Fig. S4*C*). We also tested the self-renewal capability of $Prdm16^{-/-}$ fetal liver HSCs by serial transplantation. Interestingly, all primary recipients of 2×10^6 $Prdm16^{-/-}$ fetal liver cells were viable at 4 mo posttransplantation. However, upon secondary transplantation, the recipients of $Prdm16^{-/-}$ fetal liver cells started dying at 3 mo after transplantation and did not survive beyond 10 mo, while recipients of wild-type fetal liver cells remained healthy (Fig. 1*D*). Taken together, these results suggest that the loss of *Prdm16* negatively affects the self-renewal of fetal liver HSCs.

Deletion of *Prdm16* in Adult Mice Leads to Gradual Reduction of LT-HSCs due to Self-Renewal Defects. In contrast to the highly proliferative fetal liver HSCs, adult LT-HSCs in the bone marrow are mostly quiescent (18). Upon hematopoietic injury or stress, for example, massive bleeding, LT-HSCs exit quiescence and contribute significantly to the production of more-mature hematopoietic cells (19). The role of *Prdm16* in adult HSCs remains unclear, as previous studies disrupted the gene before the establishment of these cells in the bone marrow (12–14). To answer this question, we bred $Prdm16^{cko/cko}$ mice with the IFN-inducible *Mx1-Cre*$^{tg/+}$ mice to generate adult $Prdm16^{cko/cko}$;*Mx1-Cre*$^{tg/+}$ and control $Prdm16^{cko/cko}$;*Mx1-Cre*$^{+/+}$ mice and analyzed their HSC compartments after inducing *Prdm16* deletion by polyinosinic–polycytidylic acid (pIpC) injections (*SI Appendix*, Fig. S5). At 2 mo post pIpC injections, the percentages of LT-HSCs and ST-HSCs in 8- to 12-wk-old $Prdm16^{cko/cko}$;*Mx1-Cre*$^{tg/+}$ mice were significantly reduced in comparison to control mice, whereas the percentage of MPPs was increased (Fig. 2*A*). Similar changes also were observed at 4 mo without detection of any significant changes in total bone marrow cellularity (*SI Appendix*, Fig. S6). These data suggest that deletion of *Prdm16* in adult bone marrow leads to a gradual but not acute loss of HSCs in our model, potentially due to their failure to self-renew. In order to determine that the reduction was intrinsic to the HSCs and not due to confounding effects from the microenvironment, we transplanted bone marrow cells from control mice and $Prdm16^{cko/cko}$;*Mx1-Cre*$^{tg/+}$ into lethally irradiated *C57BL/6-Ly5.2* mice. We subsequently induced *Prdm16* deletion at 2 mo posttransplantation and analyzed donor HSCs at 4 mo afterward (Fig. 3*A*). *Prdm16* deletion in the transplanted cells led to a reduction in the percentages of donor LT-HSCs and ST-HSCs and an increase in the percentage of donor MPPs, confirming an intrinsic role for *Prdm16* in adult HSCs (Fig. 3*B*). In addition, *Prdm16* deletion did not have any obvious effects on hematopoietic development in the periphery, since no difference was found in the percentages of donor-derived myeloid or lymphoid cells in the recipient mice at 2 mo after pIpC injections (*SI Appendix*, Fig. S7). Since *Prdm16* deletion in primary or transplanted animals did

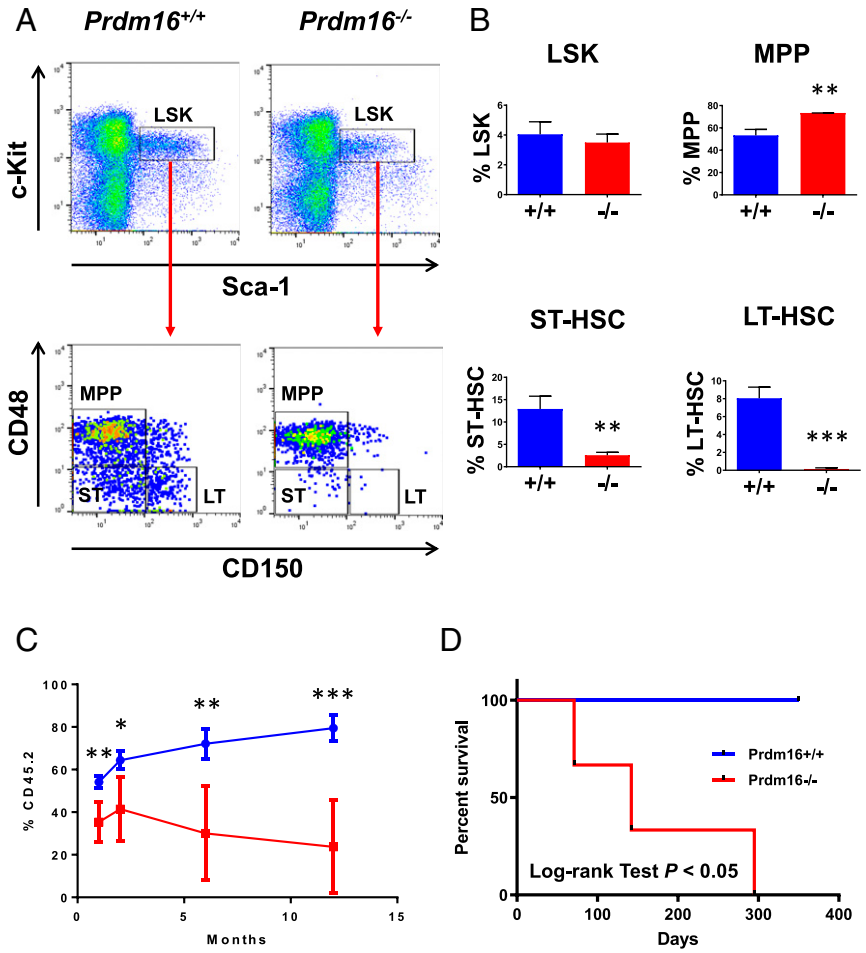

Fig. 1. Significant reduction in fetal liver HSCs after *Prdm16* deletion. (*A*) Representative FACS analysis of LSK compartments including LT-HSC (LT), ST-HSC (ST), and MPP in fetal livers of e18.5 $Prdm16^{-/-}$ versus $Prdm16^{+/+}$ embryos. (*B*) Quantification of results in *A* ($n = 3$ for each group). The frequencies (mean ± SD) of LSK cells in total bone marrow nucleated cells and of LT-HSC/ST-HSC/MPP populations in LSK cells are shown. (*C*) Competition of 1×10^6 e18.5 $Prdm16^{-/-}$ or $Prdm16^{+/+}$ fetal liver cells against equal number of wild-type *C57BL/6-Ly5.2* bone marrow cells in lethally irradiated *C57BL/6-Ly5.2* recipient mice. The frequencies (mean ± SD) of fetal liver cells ($CD45.2^+$) in peripheral blood of recipient mice at 1, 2, 6, and 12 mo after transplantation are shown ($n = 5$ for each fetal liver genotype). (*D*) Survival curves of irradiated *C57BL/6-Ly5.2* mice receiving 1×10^6 bone marrow cells from primary recipient mice of e18.5 $Prdm16^{-/-}$ or $Prdm16^{+/+}$ fetal liver cells ($n = 3$ for each genotype). $^*P < 0.05$; $^{**}P < 0.01$; $^{***}P < 0.001$.

not lead to acute bone marrow failure, we performed serial transplantations to test the self-renewal capability of *Prdm16*-deleted HSCs at 4 mo after pIpC injections. Interestingly, recipients of $Prdm16^{cko/cko};Mx1\text{-}Cre^{tg/+}$ bone marrow survived secondary transplantation despite significant reduction in LT-HSCs but succumbed to bone marrow failure in a tertiary transplantation (Fig. 3 *C* and *D*). Overall, these data strongly suggest that *Prdm16* is an important intrinsic regulator for the self-renewal of adult LT-HSCs but not their differentiation into mature hematopoietic lineages.

Further Reduced Self-Renewal Capability of *Prdm16*-Deficient Adult HSCs under Stress. We also examined the self-renewal capability of *Prdm16*-deficient adult HSCs by performing competitive repopulation assay. No significant difference in reconstitution was detected between bone marrow cells from $Prdm16^{cko/cko};Mx1\text{-}Cre^{+/+}$ and $Prdm16^{cko/cko};Mx1\text{-}Cre^{tg/+}$ mice (*SI Appendix*, Fig. S8), potentially due to the slow and gradual reduction in adult LT-HSCs upon *Prdm16* deletion. We therefore tested whether stress could accelerate their loss by injecting the recipient mice with three separate doses of 5-fluorouracil (5-FU) 2 wk apart after inducing *Prdm16* deletion (Fig. 4*A*). Since 5-FU is toxic for actively proliferating hematopoietic cells, quiescent LT-HSCs are forced to divide in order to respond to their loss (20). Analysis of peripheral blood from the recipients of $Prdm16^{cko/cko};Mx1\text{-}Cre^{+/+}$ or control $Prdm16^{cko/cko};Mx1\text{-}Cre^{tg/+}$ bone marrow before pIpC injections showed that the reconstitution by donor (CD45.2) and competitor (CD45.1) cells was essentially equal between the groups (Fig. 4*B*). In contrast, at 1 mo post pIpC injections, the percentage of $Prdm16^{cko/cko};Mx1\text{-}Cre^{tg/+}$ donor cells in recipient mice was notably lower than that of $Prdm16^{cko/cko};Mx1\text{-}Cre^{+/+}$ cells, suggesting that repeated stress following loss of *Prdm16* significantly reduces their ability to compete with wild-type HSCs (Fig. 4*B*). At 2 and 6 mo, the difference increased further (Fig. 4*B*), with significant reductions in granulocytes ($CD45.2^+Gr\text{-}1^+$) and macrophages ($CD45.2^+Mac\text{-}1^+$) (Fig. 4*C*). In addition, analysis of the bone marrow of these mice at 6 mo showed a drastic reduction in the number of *Prdm16*-deleted LT-HSCs, demonstrating that the cells were efficiently exhausted and outcompeted after 5-FU–induced stress (*SI Appendix*, Fig. S9).

Increased Cycling in Adult LT-HSCs Lacking *Prdm16*. Loss of *Prdm16* resulted in a significant decrease in the self-renewal capability of adult LT-HSCs, suggesting that *Prdm16* deletion could be decreasing their survival and/or causing the cells to differentiate, possibly by reducing their quiescence. To determine the cell cycle

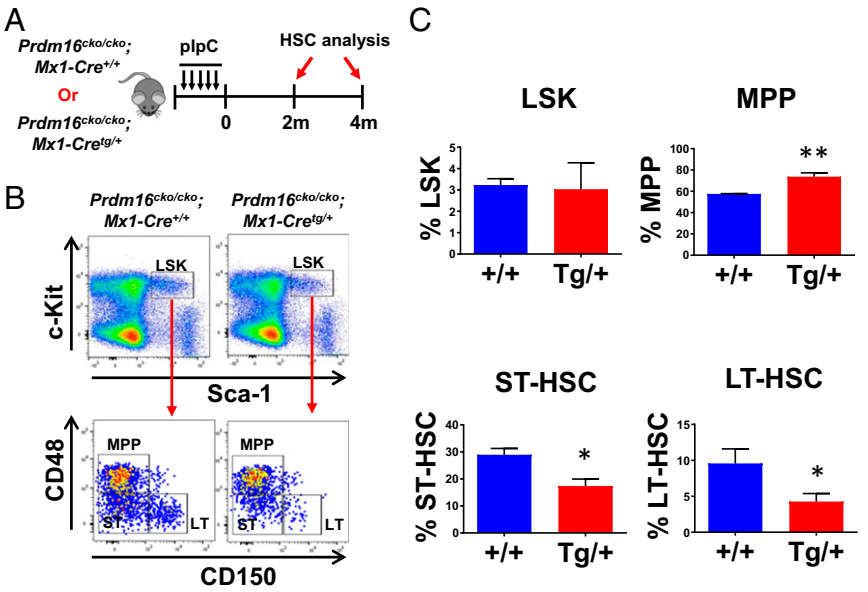

Fig. 2. Conditional *Prdm16* deletion induces gradual and significant reduction in adult HSCs. (*A*) Schematic overview of *Prdm16* deletion induction in adult *Prdm16*$^{cko/cko}$;*Mx1-Cre*$^{tg/+}$ mice. (*B*) Representative FACS analysis of LSK compartments including LT-HSC (LT), ST-HSC (ST), and MPP in bone marrow of *Prdm16*$^{cko/cko}$;*Mx1-Cre*$^{tg/+}$ versus *Prdm16*$^{cko/cko}$;*Mx1-Cre*$^{+/+}$ mice at 2 mo after pIpC injections. (*C*) Quantification of results in *B* ($n = 4$ for each group). The frequencies (mean ± SD) of LSK cells in total bone marrow nucleated cells and LT-HSC/ST-HSC/MPP populations in LSK cells are shown. *$P < 0.05$; **$P < 0.01$.

status and survival of LT-HSCs upon *Prdm16* loss, we performed cell cycle analysis by Bromodeoxyuridine (BrdU) incorporation (21) and apoptosis analysis by Annexin V staining (22) on LT-HSCs from *Prdm16*$^{cko/cko}$;*Mx1-Cre*$^{+/+}$ and *Prdm16*$^{cko/cko}$;*Mx1-Cre*$^{tg/+}$ mice at 2 mo after pIpC injections. The BrdU analysis demonstrated significantly increased cycling of LT-HSCs in the pIpC-treated *Prdm16*$^{cko/cko}$;*Mx1-Cre*$^{tg/+}$ mice compared to control mice (Fig. 5 *A* and *B*). In contrast, no significant increase in

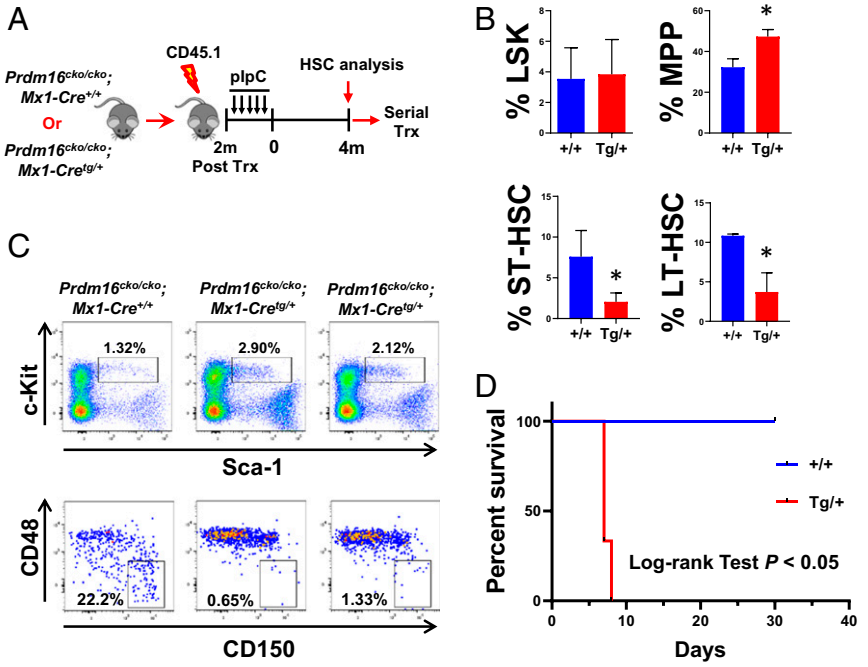

Fig. 3. Reduction in adult HSCs induced by *Prdm16* deletion is cell-intrinsic. (*A*) Schematic overview of *Prdm16* deletion in a transplantation assay to analyze the intrinsic role of *Prdm16* in LT-HSCs. Lethally irradiated *C57BL/6-Ly5.2* recipient mice were transplanted with 1×10^6 bone marrow cells from *Prdm16*$^{cko/cko}$;*Mx1-Cre*$^{tg/+}$ or *Prdm16*$^{cko/cko}$;*Mx1-Cre*$^{+/+}$ mice. After a 2-mo recovery period, recipient mice were injected with pIpC every other day for a total of five injections and analyzed 4 mo post pIpC injections. (*B*) The frequencies (mean ± SD) of CD45.2$^+$LSK cells in CD45.2$^+$ bone marrow nucleated cells and LT-HSC/ST-HSC/MPP populations in CD45.1$^+$LSK cells in primary recipient mice at 4 mo after pIpC injections are shown ($n = 5$ for each genotype). (*C*) Representative FACS analysis of CD45.2$^+$LSK and CD45.2$^+$LT-HSC populations in secondary recipient mice at 4 mo posttransplantation. (*D*) Survival curves of irradiated tertiary recipient mice receiving 1×10^6 bone marrow cells from secondary recipients ($n = 5$ for each genotype). *$P < 0.05$.

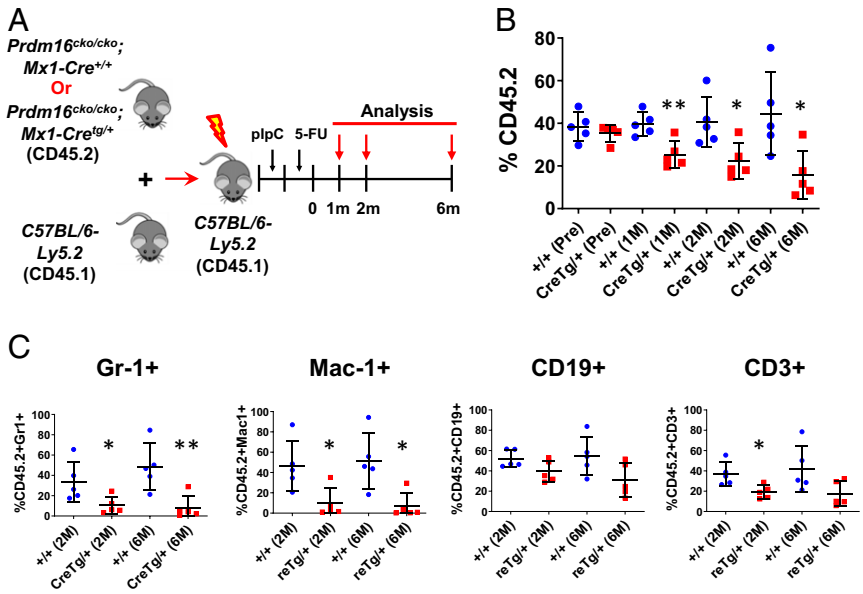

Fig. 4. Competitive reconstitution capability of *Prdm16*-deficient HSCs was significantly reduced after 5-FU treatments. (*A*) Schematic overview of a competitive reconstitution assay to analyze the intrinsic role of *Prdm16* in LT-HSCs. Lethally irradiated *C57BL/6-Ly5.2* mice were transplanted with 1×10^6 bone marrow cells from *Prdm16*$^{cko/cko}$;*Mx1-Cre*$^{tg/+}$ or *Prdm16*$^{cko/cko}$;*Mx1-Cre*$^{+/+}$ mice plus 1×10^6 CD45.1$^+$ competitor bone marrow cells from healthy *C57BL/6-Ly5.2* mice. After a 2-mo recovery period, mice were treated with five pIpC injections followed by three 5-FU injections 2 wk apart and analyzed at 1, 2, and 6 mo post 5-FU injections for donor (CD45.2+) reconstitution. (*B*) Frequencies (mean ± SD) of CD45.2$^+$ cells in peripheral blood of recipient mice at indicated time points after 5-FU treatments. (*C*) Frequencies (mean ± SD) of CD45.2$^+$Gr-1$^+$, CD45.2$^+$Mac-1$^+$, CD45.2$^+$CD19$^+$, and CD45.2$^+$CD3$^+$ in peripheral blood of recipient mice at indicated time points after 5-FU treatments ($n = 5$ for each genotype). *$P < 0.05$; **$P < 0.01$.

Annexin V staining was detected in *Prdm16*-deleted LT-HSCs upon induction of *Cre* expression (Fig. 5*C*). Taken together, our data suggest that the reduced self-renewal capability and premature differentiation of *Prdm16*-deleted adult LT-HSCs is likely due to their decreased ability to maintain quiescence.

Deletion of *Prdm16* Decreases the Expression of Genes Critical for LT-HSC Quiescence and Self-Renewal. To investigate the mechanism by which *Prdm16* regulates LT-HSC function, we performed RNA sequencing (RNA-seq) analysis of sorted LT-HSCs from *Prdm16*$^{cko/cko}$;*Mx1-Cre*$^{tg/+}$ and *Prdm16*$^{cko/cko}$;*Mx1-Cre*$^{+/+}$ mice treated with pIpC (Fig. 6*A*). To minimize short-term effects of pIpC on gene expression, these cells were purified at 5 wk after the last pIpC injection for the analysis. Deletion of *Prdm16* was confirmed by genotyping and sequencing reads mapped to the locus (*SI Appendix*, Fig. S10). We found that 1,578 genes were differentially expressed between the two populations, with 564 genes down-regulated in the *Prdm16*-deleted LT-HSCs and 1,014 genes up-regulated using 1.5-fold change in gene expression as the cutoff (Fig. 6*B* and Dataset S1). As expected from the defective maintenance of these cells after *Prdm16* deletion, gene set enrichment analysis (GSEA) demonstrated up-regulation of gene sets down-regulated in normal HSCs and leukemia stem cells and gene signatures associated with more differentiated cell types (Fig. 6*C* and *SI Appendix*, Fig. S11). Consistent with the increased proliferation of these cells upon *Prdm16* loss, genes associated with cell cycle arrest were found to be mostly down-regulated upon *Prdm16* deletion (Fig. 6*D*). Importantly, several genes previously known to be critical for maintaining the quiescence and self-renewal function of HSCs were significantly down-regulated in *Prdm16*-deleted cells, including *Fos*, *Egr1*, *Cdkn1a*, and *Fosb* (Fig. 6*E* and *SI Appendix*, Fig. S12) (1, 23–25). However, we did not detect any significant correlation with gene signatures associated with senescence and oxidative stress previously linked to *Prdm16* disruption.

Cell Cycle Regulators *Cdkn1a* and *Egr1* Are Direct Targets of *Prdm16*. Cell cycle control plays an important role in maintaining the self-renewal function of adult LT-HSCs. Our cell cycle analysis of

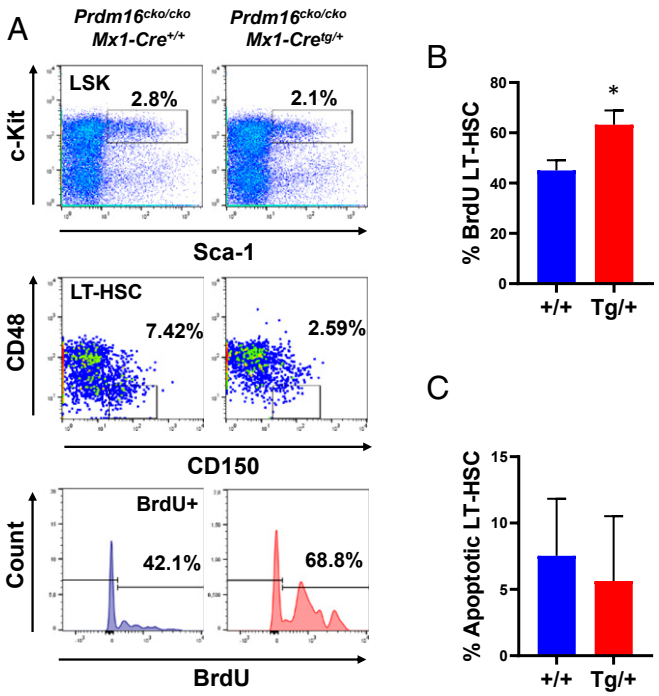

Fig. 5. *Prdm16* deletion promoted cycling of LT-HSCs without affecting apoptosis. (*A*) Representative cell cycle analysis of LT-HSCs in *Prdm16*$^{cko/cko}$;*Mx1-Cre*$^{tg/+}$ or *Prdm16*$^{cko/cko}$;*Mx1-Cre*$^{+/+}$ mice after pIpC injections. (*B*) Quantification of results in *A* ($n = 4$ for each group). (*C*) Frequencies of Annexin V positive apoptotic LT-HSCs in *Prdm16*$^{cko/cko}$;*Mx1-Cre*$^{tg/+}$ or *Prdm16*$^{cko/cko}$;*Mx1-Cre*$^{+/+}$ mice after pIpC injections ($n = 4$ for each group). *$P < 0.05$.

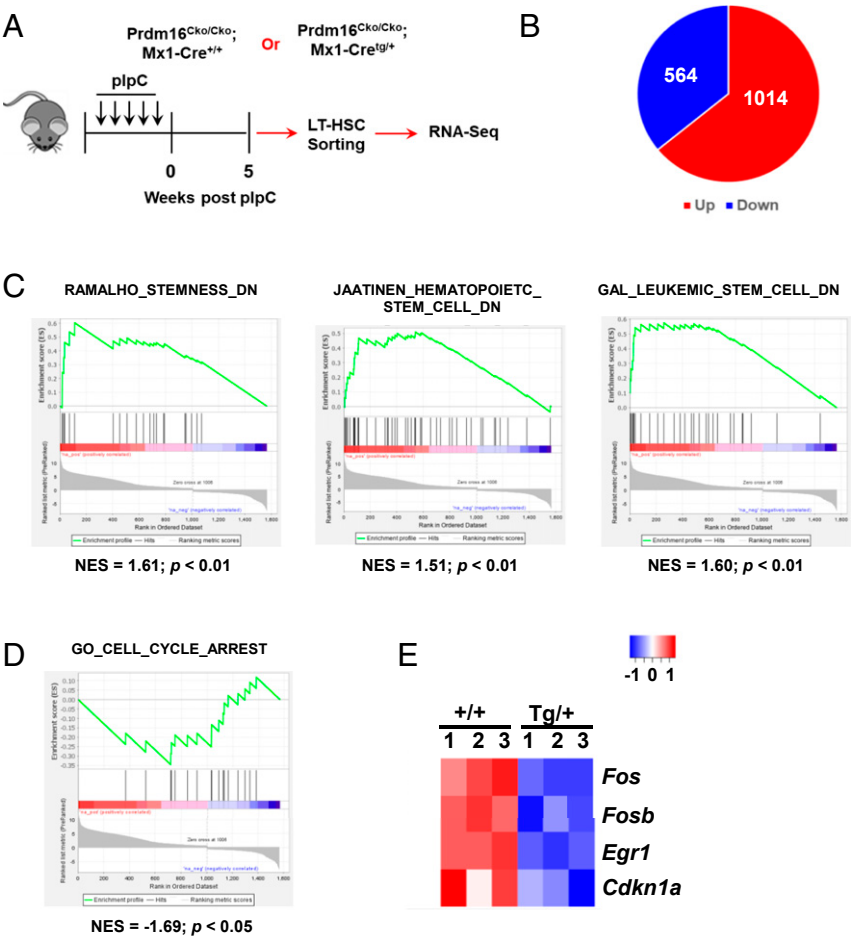

Fig. 6. RNA-seq analysis of LT-HSCs before and after *Prdm16* deletion. (*A*) Schematic overview of collection of LT-HSCs for RNA-seq analysis. (*B*) Pie chart showing the numbers of differentially expressed genes induced by *Prdm16* deletion. (*C*) GSEA analysis of differentially expressed genes in LT-HSCs after *Prdm16* deletion using gene sets down-regulated in stem cells. (*D*) GSEA analysis of differentially expressed genes in LT-HSCs after *Prdm16* deletion using a gene set associated with cell cycle arrest. (*E*) Heat map showing reduced expression of regulator genes of HSC quiescence and maintenance after *Prdm16* deletion.

Prdm16-deleted adult LT-HSCs suggests that *Prdm16* is a critical regulator of quiescence in these cells. Among genes whose expression was significantly changed by *Prdm16* deletion, both *Cdkn1a* and *Egr1* have been shown to be important for cell cycle regulation and maintenance of HSCs in vivo, by gene targeting studies (1, 23). Analysis of the *Cdkn1a* and *Egr1* locus using the Genomatix software revealed several potential PRDM16 binding sites, suggesting that both could be direct transcriptional targets of PRDM16. To test this hypothesis, we performed chromatin immunoprecipitation (ChIP) analysis in BM2 myeloid progenitor cells which were immortalized due to retroviral insertional activation of *Prdm16* (10). Significant PRDM16 binding was readily detected at regions containing potential PRDM16 binding sites (Fig. 7), suggesting that both *Cdkn1a* and *Egr1* represent direct targets of PRDM16. Taken together, our data suggest that *Prdm16* plays a critical role in maintaining quiescence of adult LT-HSCs by directly regulating *Cdkn1a* and *Egr1* expression.

Discussion

In this study, we found that *Prdm16* is a critical regulator of adult HSC quiescence but is dispensable for the generation of downstream progenitors and mature cells. We showed that loss of *Prdm16* in adult HSCs leads to increased cycling and gradual loss of the cells over time. We also showed that HSC loss was accelerated upon 5-FU–induced stress, underscoring an increased importance of *Prdm16* for HSCs under stress conditions. Our data further uncovered several key downstream targets of *Prdm16* that likely contribute to its regulation of HSC dormancy. We additionally identified the CDK inhibitor gene *Cdkn1a* and the transcription factor gene *Egr1* as direct transcriptional targets of *Prdm16*.

Prdm16 is likely a specific regulator of HSCs, which could explain why the hematopoietic phenotype of our adult mouse model is only acute under severe stress such as serial transplantation or serial 5-FU treatments. A recent study has suggested that hematopoiesis in the adult is mostly maintained by short-term HSCs and MPPs but not LT-HSCs (26). LT-HSCs rarely contribute to the hematopoietic pool except under stress, for example, with 5-FU injections. Therefore, it is challenging to detect a phenotype in adult HSCs that have lost *Prdm16* expression, since the gene appears to be critical only for that compartment. Many knockout models claiming an HSC phenotype also have significant effects on downstream progenitors, which makes the phenotype more severe (27, 28). It could be argued that, in those cases, it is difficult to distinguish between true HSC defects in vivo and a failure of more committed progenitors.

According to our data, apoptosis was not affected in adult LT-HSCs after *Prdm16* deletion, whereas cycling was significantly increased compared to controls. Stringent regulation of the cell cycle is critical for maintaining adult LT-HSCs in a quiescent state and in allowing self-renewal to occur to preserve the HSC

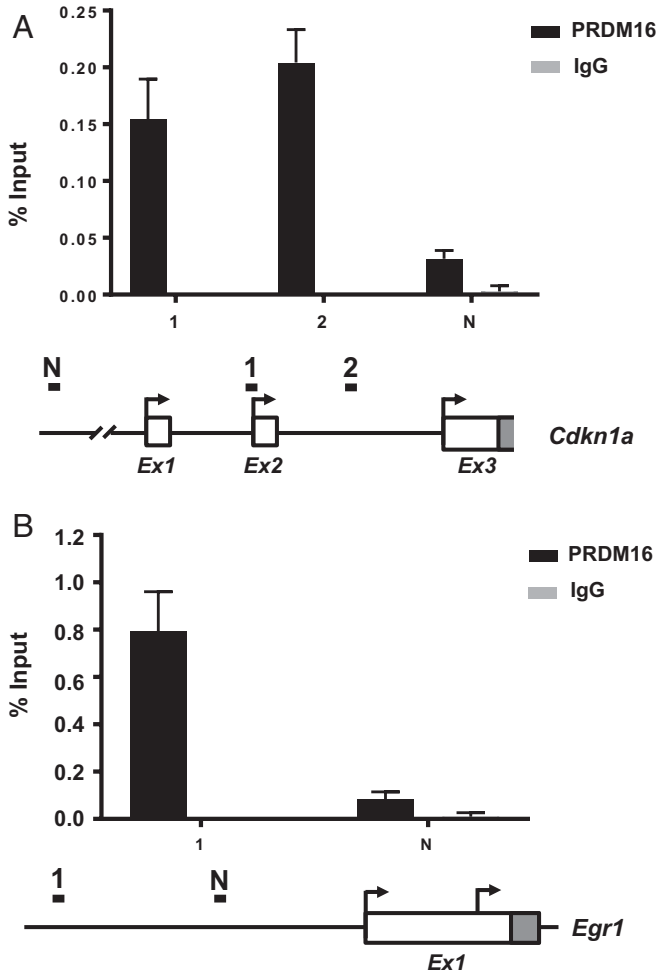

Fig. 7. *Cdkn1a* and *Egr1* represent direct targets of *Prdm16*. ChIP analysis of regions of (*A*) *Cdkn1a* or (*B*) *Egr1* locus containing predicted PRDM16 binding sites (1, 2) and negative control regions (N) in BM2 myeloid progenitors using a PRDM16-specific antibody and control IgG (*Upper*, mean ± SD). Diagrams of tested region of *Cdkn1a* and *Egr1* locus are also shown (*Lower*). Locations of PCR amplicons are indicated as black bars. Transcriptional start sites are indicated as arrows. Exons are indicated as white boxes with coding regions highlighted in gray.

pool (29). It is therefore likely that increased cycling of adult LT-HSCs upon *Prdm16* deletion is responsible for their gradual loss through differentiation. Fetal liver HSCs, unlike adult HSCs, proliferate extensively. It is also possible that *Prdm16* loss in fetal liver HSCs could further increase their proliferation, leading to an accelerated exhaustion of these cells. In line with these phenotypic findings, one of the significantly down-regulated genes upon *Prdm16* loss is the CDK inhibitor *Cdkn1a*, which maintains LT-HSCs as quiescent by preventing the cell from exiting the G0 phase of the cell cycle (1). Another significantly down-regulated gene is *Egr1*, loss of which has been shown to increase cycling of LT-HSCs, in part, by decreasing *Cdkn1a* expression (23). Our ChIP results in BM2 cells further suggest that both are direct targets of PRDM16. It will be important to validate the role of *Cdkn1a* in *Prdm16*-mediated regulation of LT-HSC quiescence by restoring its expression in *Prdm16*-deleted LT-HSCs; however, such experiments will be difficult to perform due to the need to precisely control the level of *Cdkn1a* expression. Overexpression of *Cdkn1a* will likely cause a complete block in the proliferation of LT-HSCs, rendering the detection of their engraftment difficult.

Both our *Prdm16* germline and conditional knockout models displayed less severe hematopoietic phenotypes than previously reported models. Our germline knockout model recapitulates the previously described gene trap model in regard to the perinatal lethality, cleft palate development, loss of phenotypic fetal liver HSCs, and lack of significant changes in mature blood cell numbers (13, 14). However, our transplantation studies, where the intrinsic function of HSCs is measured, did not show the same acute phenotype as the previous gene trap and knockout models where *Prdm16*-deficient fetal liver cells competed very poorly with wild-type BM cells. Similarly shown by competition assay, the adult HSC defect in our conditional knockout model is also significantly less severe than a recently reported conditional model (12). One main reason for these differences could be our *Prdm16* targeting strategy, which likely results in a more complete ablation of *Prdm16* expression. Based on mouse expressed sequence tags mapped to the *Prdm16* locus (genome.ucsc.edu), shorter *Prdm16* transcripts potentially initiating from the region between exons 11 and 12 likely exist. Indeed, by performing 5′ rapid amplification of complementary DNA (cDNA) ends (5′ RACE) in mouse LSK cells, we have identified two such novel transcripts of *Prdm16*, both predicted to produce a significantly shorter PRDM16 isoform (*SI Appendix*, Fig. S13). These mRNAs should be inactivated by Cre recombination in our model, while likely remaining intact in the previously reported gene trap and conditional models. Although the function of this significantly shorter isoform is unclear, it is possible that it may normally antagonize the activity of the two longer isoforms, due to its truncated nature. Therefore, the loss of just the longer isoforms in previous models may disrupt a critical balance, which may translate into a more severe phenotype. Future studies will be needed to clarify the function of this shorter isoform. Another possibility may also contribute to the phenotypic difference between our conditional model using *Mx1-Cre* and the previously reported conditional model using *Vav-Cre*. As *Vav-Cre* is expressed in fetal liver HSCs, it is possible that loss of *Prdm16* in these cells may affect their transition into fully functional adult HSCs.

Materials and Methods

Mice. All mice were maintained in the animal facility of Laboratory of Animal Medicine at Uniformed Services University of the Health Sciences (USUHS). Female *C57BL/6-Ly5.2* mice (Charles River, 8 wk to 12 wk old) were used as recipients for all transplantation experiments. All mouse experiments were carried out according to protocols approved by USUHS Institutional Animal Care and Use Committee.

Generation of *Prdm16* Conditional and Knockout Alleles in Mice. A 129 bacterial artificial chromosome (BAC) library (CT7, Invitrogen) was screened with a *Prdm16* genomic probe to identify a BAC clone containing the *Prdm16* genomic locus (clone no. 264O8). Two targeting constructs were generated to insert one *loxP* site into intron 5 and another in intron 12 of *Prdm16*. Two fragments (7.9 and 8.4 kb) containing intron 5 and intron 12 of *Prdm16*, respectively, were first retrieved from the BAC clone in EL350 cells through recombineering into an ES cell targeting vector PL253 as previously described (30). A *loxP* plus *Frt*-flanked neocassette was targeted to the resulting intron 5 retrieval construct in EL350 cells through recombineering. First, a targeting cassette containing *Pgk-em7-neo* flanked by homology arms to intron 5 of *Prdm16* was constructed in PL451. The homology arms are PCR amplified using the following primers: 5′ arm sense, 5′-CGG CGG CCG CGT ACC CAC ACT GAC AAG TAG-3′; 5′ arm antisense, 5′-CGC GGG ATC CAG CTA GCC TGC CTG GAG AGA GAA CAC C-3′; 3′ arm sense, 5′-CGC GGA ATT CAA GCT TGG GTG AAA GCT GAA GGG CCT-3′; 3′ arm antisense, 5′-CGC GGT CGA CTG AGC AAA GTC AGG CTC CTC-3′. The homology arms were sequence verified, restriction digested, and cloned into PL451 via four-way ligation. The targeting cassette was released by *NotI*/*SalI* double digest and targeted through coelectroporation into heat shock-induced EL350 cells. To insert the second *loxP* site in intron 12 of *Prdm16*, a targeting cassette containing *frt5-Pgk-Em7-blast-frt5-loxP* flanked by homology arms to targeting site was constructed in a modified version of PL451. Homology arms were amplified using the following primers: 5′ arm sense, 5′-CGG CGG CCG

Cdkn1a-1	5′ GCC GCG GTG TCA GAG TCT AG 3′
	5′ CGA AGC TCT CAC CTC TGA ATG TC 3′
Cdkn1a-2	5′ TTT AGG AAG CCT GGG CTC ATC 3′
	5′ GGT GGA GAG AGG AGA GGA AAG G 3′
Cdkn1a-N	5′ GGG AAG GTA GGA AAG GAT ATT TGG 3′
	5′ CCG CCC GTC GAC CAT 3′
Egr1-1	5′ CTC TCA GCC ATC GGA AAG TGT 3′
	5′ TAG GGC TCA GGA AGT GAC TCT CTT 3′
Egr1-N	5′ AGC CTG GGC TGA ATC AAA AG 3′
	5′ TCA GTG GTA GGA AAT CAG AGA AGA GA 3′

CGG AGC AGC CAT ACA GGT AG-3′; 5′ arm antisense, 5′-CGC GGG ATC CCA GGC TCT CTC ACA TCC TCT-3′; 3′ arm sense, 5′-CGC GGA ATT CTC TCC TGT ATC CAA AGT GTC-3′; 3′ arm antisense, 5′-CGC GGT CGA CTA GCC CCT CGT TTT TGA CAC-3′. The targeting cassette was released by *Not*I/*Sal*I double digest and targeted similarly as described above. The intron 5 targeting vector after linearization by *Not*I digestion was first electroporated into 129-derived CJ7 ES cells, using standard procedures. G418 (180 μg/mL) and Ganciclovir (2 μM) double-resistant clones were analyzed by Southern blotting hybridization, using both 5′ and 3′ external probes. One of the correctly targeted clones was expanded and subsequently electroporated with the intron 12 targeting vector linearized also by *Not*I digestion. Clones resistant to Blasticidin (12.5 μg/mL) and Ganciclovir (2 μM) were also analyzed by Southern blotting hybridization, using both 5′ and 3′ external probes. External probes were PCR amplified using the following primers: *loxP*1 5′ probe, sense, 5′-CCT AAG GTG GTC CTT GAG AG-3′; *loxP*1 5′ probe, antisense, 5′-CAA CTT TCC CGG CTG AAC AG-3′; *loxP*1 3′ probe (*loxP*2 5′ probe), sense, 5′-TCT AAG TCT GCT CCC TGA TG-3′; *loxP*1 3′ probe (*loxP*2 5′ probe), antisense, 5′-TTT CCC TCT CTG GAG CCT TG-3′; *loxP*2 3′ probe, sense, 5′-TCT CTG CTG TTA GGG CCA AC-3′; *loxP*2 3′ probe, antisense, 5′-ATC AAG TGC CGT GGG AGC TG-3′. The *loxP*1 3′ probe (*loxP*2 5′ probe) was also used after the second targeting and *Hpa*I/*Mfe*I double digestion of DNA to identify ES clones with the two *loxP* sites targeted to the same *Prdm16* locus. Correctly targeted clones were then injected into C57BL/6 blastocysts using standard procedures, and resulting chimeras were mated with C57BL/6 females to obtain germline transmission of the targeted allele. A *Prdm16* conventional knockout and a conditional allele were subsequently generated by breeding mice carrying the targeted allele with *ACTB-Cre* and *ACTB-Flpe* mice, respectively. Both heterozygous knockout and conditional mice were backcrossed to C57BL/6J mice for 7 generations.

Bone Marrow Transplantation. For transplantation, fetal liver (e18.5) or BM cells were injected into the tail vein of each lethally irradiated (1,100 rads from ^{137}Cs source) *C57BL/6-Ly5.2* female mouse without supporting bone marrow cells from unirradiated C57BL/*6-Ly5.2*mice. Retroorbital bleeding was performed at 1, 2, and 6 mo to analyze the short-term and long-term engraftment of the donor cells by fluorescence-activated cell sorting (FACS). For secondary or tertiary transplantation, 1×10^6 cells from bone marrow of primary or secondary recipients were injected into lethally irradiated secondary or tertiary recipients without supporting bone marrow cells. To induce *Prdm16* deletion in conditional cells at 2 mo after transplantation, recipient mice were injected with five injections of 400 μg of pIpC (Calbiochem) dissolved in phosphate-buffered saline at 2-d intervals.

Flow Cytometry. Flow cytometry analyses of mouse fetal tissues (liver and thymus) and adult tissues (peripheral blood and bone marrow) were performed using BD LSRII flow cytometer. After sample collection and ACK lysis of red blood cells, cells were blocked by incubation with anti-FcγR-II/III and subsequently stained with antibodies against markers for myeloid (Gr-1, Mac-1), erythroid (Ter-119), B (CD19), and T (CD3) lineages (Biolegend). Dead cells were excluded by staining with Sytox Blue (Invitrogen). For analysis of LT-HSCs (Lin$^-$Sca-1$^+$c-Kit$^+$CD48$^-$CD150$^+$), ST-HSCs (Lin$^-$Sca-1$^+$c-Kit$^+$CD48$^-$CD150$^-$), and MPPs (Lin$^-$Sca-1$^+$c-Kit$^+$CD48$^+$CD150$^-$), after ACK lysis of red blood cells, lineage-positive cells were first labeled by incubation with a mixture of purified rat anti-mouse antibodies specific for Gr-1, Mac-1 (not included for fetal liver cells), CD4, CD8, B220, CD127, and Ter-119, and subsequently labeled by incubation with sheep anti-rat PE-Cy5 (Invitrogen). The Lin$^-$ cells were then stained with allophycocyanin (APC)-conjugated anti-mouse Sca-1 (D7, Biolegend), APC-eFluor 780-conjugated anti-mouse c-Kit (ACK2, eBioscience), PE-Cy7-conjugated anti-mouse CD150 (TC15-12F12.2, Biolegend), biotinylated anti-mouse CD48 (HM48-1, Biolegend) antibodies, and Streptavidin-Pacific Orange (Invitrogen). All samples were analyzed using a BD LSRII flow cytometer, and data were analyzed using FlowJo software.

Cell Cycle and Apoptosis Analysis. Cell cycle status of LT-HSC was analyzed in *Prdm16$^{cko/cko}$;Mx1-Cre$^{+/+}$* and *Prdm16$^{cko/cko}$;Mx1-Cre$^{tg/+}$* mice by BrdU incorporation as previously described (31). Briefly, 2 mo post pIpC injections (5×), mice were injected intraperitoneally with 5 mg of BrdU and maintained on 1 mg/mL BrdU in the drinking water for 72 h. Bone marrow cells were subsequently harvested and stained with antibodies against lineage markers, c-kit, Sca-1, CD150, and CD48 for LT-HSC detection and analyzed using the fluorescein isothiocyanate (FITC) BrdU Flow Kit (BD Pharmingen). Apoptosis in LT-HSC was analyzed 2 mo post pIpC injections using the FITC Annexin-V staining kit (BD Pharmingen) according to the manufacturer's instructions.

RNA-seq and Bioinformatics Analysis. Bone marrow was harvested from adult (8 wk to 12 wk old) Prdm16$^{cko/cko}$;Mx1-Cre$^{+/+}$ and Prdm16$^{cko/cko}$;Mx1-Cre$^{tg/+}$ (five each genotype) 5 wk post pIpC injections for LT-HSCs (Lin$^-$Sca-1$^+$c-Kit$^+$CD48$^-$CD150$^+$) sorting. LT-HSCs were sorted from pooled bone marrow directly into 100 μL of RNA lysis buffer (from PicoPure RNA Isolation Kit, Thermo Cat. No. KIT0204) in three technical replicates for each genotype and stored at −80 °C. Low-input RNA purification, library generation, and Illumina sequencing were performed at Cofactor Genomics. The RNA integrity number values for purified RNA were ≥9. Sequencing produced ∼30,000,000 single-end reads per sample with minimum read length of 1 × 75 bp. Processed and trimmed FASTQ sequencing files were uploaded and analyzed using the Galaxy platform (https://usegalaxy.org). Briefly, to ensure sequence quality, FASTQ files were analyzed by FastQC and then aligned to the mouse genome (mm10) using HISAT2. Read counts were determined from aligned binary alignment map files with FeatureCounts, and differential gene expression was performed using the Limma Bioconductor package with a cutoff of $P < 0.05$ and 1.5-fold change. Heatmaps were generated from normalized count files using Heatmap2. GSEA was performed using the GSEA v4.0.3 application (https://www.gsea-msigdb.org/gsea/index.jsp).

ChIP. ChIP analyses were performed using ChIP-IT Express kit (Active Motif). Immunoprecipitations were performed using sheep anti-PRDM16 antibody (10E2, #5356, Cell Signaling Technologies) and sheep IgG (#P120-101, Bethyl Laboratories). Chromatin DNA was purified using MinElute PCR Purification Kit (QIAGEN) and quantified by real-time PCR. The following locus-specific primers were used:

Real-Time RT-PCR. Total RNA was extracted using RNAeasy Plus mini kit (Qiagen). For real-time RT-PCR, oligo-dT-primed cDNA samples were prepared from total RNA using SuperScript III (Invitrogen), and real-time PCR analysis was performed in triplicate using SYBR green detection reagents (Invitrogen) according to the manufacturer's instructions in 20-μL final volume in 96-well plates on a QuantStudio real-time PCR system (Applied Biosystems). The cycling conditions are 50 °C for 2 min followed by 95 °C for 2 min, and then 40 cycles of 95 °C for 15 s and 60 °C for 1 min. Primer specificity was verified by sequencing PCR products and performing melting curve analysis after PCR. Relative changes in expression were calculated according to the $^{\Delta\Delta}$Ct method. Gene-specific primer sequences are as follows:

5′RACE. The 5′RACE was performed on total RNA extracted from mouse LSK cells using the SMARTer RACE 5′/3′ Kit (Takara) following user instructions.

Prdm16	5′ TCC GCG GTC AGC AAT AGC 3′
	5′ CCG ACA TGT CAG GGC TCC TA 3′
Cdkn1a	5′ CGA GAA CGG TGG AAC TTT GAC 3′
	5′ CCA GGG CTC AGG TAG ACC TT 3′
Egr1	5′ AGA CGA GTT ATC CCA GCC AAA 3′
	5′ GGT CGG AGG ATT GGT CAT GC 3′
Rpl4	5′ ATG ATG AAC ACC GAC CTT AGC A 3′
	5′ CGG AGG GCT CTT TGG ATT TC 3′

Prdm16-specific primer used for PCR amplification was: 5′ CTG GTG CCC AGG TGG TTC GTG AGC AC 3′.

Statistical Analysis. Sample sizes and animal numbers were determined by previous experiences. No samples were excluded from analyses. All data were analyzed by two-tailed Student's *t* test, except that survival curves were compared by log-rank test. The researchers were not blinded during sample collection and analysis.

Data Availability. RNA-seq data that support the findings of this study are available in the Gene Expression Omnibus (GEO) under accession number GSE154011.

ACKNOWLEDGMENTS. This work was supported by USUHS Research Accelerating Military Pediatrics Grant 310534 (Y.D.). The authors would like to thank USUHS flow cytometry core facility for assistance in data analysis. The views presented in this manuscript are those of the authors; no endorsement by USUHS or the Department of Defense has been given or should be inferred.

1. T. Cheng *et al*., Hematopoietic stem cell quiescence maintained by p21cip1/waf1. *Science* **287**, 1804–1808 (2000).
2. P. Zou *et al*., p57(Kip2) and p27(Kip1) cooperate to maintain hematopoietic stem cell quiescence through interactions with Hsc70. *Cell Stem Cell* **9**, 247–261 (2011).
3. H. Hock *et al*., Gfi-1 restricts proliferation and preserves functional integrity of haematopoietic stem cells. *Nature* **431**, 1002–1007 (2004).
4. F. Ficara, M. J. Murphy, M. Lin, M. L. Cleary, Pbx1 regulates self-renewal of long-term hematopoietic stem cells by maintaining their quiescence. *Cell Stem Cell* **2**, 484–496 (2008).
5. Y. Zhang *et al*., PR-domain-containing Mds1-Evi1 is critical for long-term hematopoietic stem cell function. *Blood* **118**, 3853–3861 (2011).
6. I. Nishikata *et al*., A novel EVI1 gene family, MEL1, lacking a PR domain (MEL1S) is expressed mainly in t(1;3)(p36;q21)-positive AML and blocks G-CSF-induced myeloid differentiation. *Blood* **102**, 3323–3332 (2003).
7. I. Pinheiro *et al*., Prdm3 and Prdm16 are H3K9me1 methyltransferases required for mammalian heterochromatin integrity. *Cell* **150**, 948–960 (2012).
8. B. Zhou *et al*., PRDM16 suppresses MLL1r leukemia via intrinsic histone methyltransferase activity. *Mol. Cell* **62**, 222–236 (2016).
9. D. C. Shing *et al*., Overexpression of sPRDM16 coupled with loss of p53 induces myeloid leukemias in mice. *J. Clin. Invest.* **117**, 3696–3707 (2007).
10. Y. Du, N. A. Jenkins, N. G. Copeland, Insertional mutagenesis identifies genes that promote the immortalization of primary bone marrow progenitor cells. *Blood* **106**, 3932–3939 (2005).
11. T. Hu *et al*., PRDM16s transforms megakaryocyte-erythroid progenitors into myeloid leukemia-initiating cells. *Blood* **134**, 614–625 (2019).
12. D. J. Corrigan *et al*., PRDM16 isoforms differentially regulate normal and leukemic hematopoiesis and inflammatory gene signature. *J. Clin. Invest.* **128**, 3250–3264 (2018).
13. S. Chuikov, B. P. Levi, M. L. Smith, S. J. Morrison, Prdm16 promotes stem cell maintenance in multiple tissues, partly by regulating oxidative stress. *Nat. Cell Biol.* **12**, 999–1006 (2010).
14. F. Aguilo *et al*., Prdm16 is a physiologic regulator of hematopoietic stem cells. *Blood* **117**, 5057–5066 (2011).
15. R. Kühn, F. Schwenk, M. Aguet, K. Rajewsky, Inducible gene targeting in mice. *Science* **269**, 1427–1429 (1995).
16. H. Ema, H. Nakauchi, Expansion of hematopoietic stem cells in the developing liver of a mouse embryo. *Blood* **95**, 2284–2288 (2000).
17. C. C. Zhang, H. F. Lodish, Murine hematopoietic stem cells change their surface phenotype during ex vivo expansion. *Blood* **105**, 4314–4320 (2005).
18. H. K. Mikkola, S. H. Orkin, The journey of developing hematopoietic stem cells. *Development* **133**, 3733–3744 (2006).
19. J. L. Zhao, D. Baltimore, Regulation of stress-induced hematopoiesis. *Curr. Opin. Hematol.* **22**, 286–292 (2015).
20. D. E. Harrison, C. P. Lerner, Most primitive hematopoietic stem cells are stimulated to cycle rapidly after treatment with 5-fluorouracil. *Blood* **78**, 1237–1240 (1991).
21. V. Jankovic *et al*., Id1 restrains myeloid commitment, maintaining the self-renewal capacity of hematopoietic stem cells. *Proc. Natl. Acad. Sci. U.S.A.* **104**, 1260–1265 (2007).
22. I. Vermes, C. Haanen, H. Steffens-Nakken, C. Reutelingsperger, A novel assay for apoptosis. Flow cytometric detection of phosphatidylserine expression on early apoptotic cells using fluorescein labelled Annexin V. *J. Immunol. Methods* **184**, 39–51 (1995).
23. I. M. Min *et al*., The transcription factor EGR1 controls both the proliferation and localization of hematopoietic stem cells. *Cell Stem Cell* **2**, 380–391 (2008).
24. S. Okada, T. Fukuda, K. Inada, T. Tokuhisa, Prolonged expression of c-fos suppresses cell cycle entry of dormant hematopoietic stem cells. *Blood* **93**, 816–825 (1999).
25. S. McKinney-Freeman *et al*., The transcriptional landscape of hematopoietic stem cell ontogeny. *Cell Stem Cell* **11**, 701–714 (2012).
26. K. Busch *et al*., Fundamental properties of unperturbed haematopoiesis from stem cells in vivo. *Nature* **518**, 542–546 (2015).
27. C. D. Jude *et al*., Unique and independent roles for MLL in adult hematopoietic stem cells and progenitors. *Cell Stem Cell* **1**, 324–337 (2007).
28. K. A. McMahon *et al*., Mll has a critical role in fetal and adult hematopoietic stem cell self-renewal. *Cell Stem Cell* **1**, 338–345 (2007).
29. L. Rossi *et al*., Less is more: Unveiling the functional core of hematopoietic stem cells through knockout mice. *Cell Stem Cell* **11**, 302–317 (2012).
30. P. Liu, N. A. Jenkins, N. G. Copeland, A highly efficient recombineering-based method for generating conditional knockout mutations. *Genome Res.* **13**, 476–484 (2003).
31. C. L. Semerad, E. M. Mercer, M. A. Inlay, I. L. Weissman, C. Murre, E2A proteins maintain the hematopoietic stem cell pool and promote the maturation of myelolymphoid and myeloerythroid progenitors. *Proc. Natl. Acad. Sci. U.S.A.* **106**, 1930–1935 (2009).